

Fano-Liouville Spectral Signatures in Open Quantum Systems

Daniel Finkelstein-Shapiro,^{1,2,3} Ines Urdaneta,^{2,3,4} Monica Calatayud,^{2,3,5} Osman Atabek,⁴ Vladimiro Mujica,¹ and Arne Keller⁴

¹*Department of Chemistry and Biochemistry, Arizona State University, Tempe AZ 85282*

²*Sorbonne Universités, UPMC Univ Paris 06, UMR 7616, Laboratoire de Chimie Théorique, F-75005, Paris, France*

³*CNRS, UMR 7616, Laboratoire de Chimie Théorique, F-75005, Paris, France*

⁴*Institut des Sciences Moléculaires d'Orsay, Bâtiment 350, UMR8214, CNRS-Université Paris-Sud, 91405 Orsay, France*

⁵*Institut Universitaire de France, France*

The scattering amplitude from a set of discrete states coupled to a continuum became known as the Fano profile, characteristic for its asymmetric lineshape and originally investigated in the context of photoionization. The generality of the model, and the proliferation of engineered nanostructured with confined states gives immense success to the Fano lineshape which is invoked whenever an asymmetric lineshape is encountered. However, many of these systems do not conform to the initial model worked out by Fano in that i) they are subject to dissipative processes and ii) the observables are not entirely analogous to the ones measured in the original photoionization experiments. In this letter, we work out the full optical response of a Fano model with dissipation. We find that the exact result for absorption, Raman, Rayleigh and fluorescence emission is a modified Fano profile where the typical lineshape has an additional Lorentzian contribution.

In a set of seminal papers spanning from 1935 and 1961, Beutler [1], Fano [2, 3] and Friederichs [4] laid the basis of the theory to describe the absorption lineshapes of atomic photoionization experiments. These lineshapes presented marked asymmetries which could not be explained by a simple Lorentzian resonance. The explanation was attributed to an interference between two photo-ionization pathways: one where the atom is ionized directly from its ground state and one where it is first excited to a higher discrete state which then ionizes (auto-ionized states). Asymmetric lineshapes can be observed in general photo-fragmentation experiments. The minimal Fano model consists in a discrete excited state coupled to a continuum set of excited states, both type of states being reachable by photo-excitation from the ground state. The resulting photo-fragmentation cross-section as a function of the excitation laser frequency ω_L is known as the Beutler-Fano or Fano profile:

$$f(\epsilon; q) = \frac{(q + \epsilon)^2}{\epsilon^2 + 1}, \quad (1)$$

where q is the ratio of the transition dipole moment of the ground-discrete and ground-continuous transitions, and $\epsilon = (E_e - \hbar\omega_L)/\gamma$ where E_e is the energy of the discrete state and $\gamma = n\pi V^2$ is the linewidth of the excited state, induced by its coupling (per unit of energy) nV^2 to the continuum set of states, n being the density of states.

Since the original photoionization experiments, the Beutler-Fano profile has been observed in an ever increasing variety of physical systems, and in particular in nanoscale structures [5, 6]. These include plasmonic nanostructures [7–9], quantum dots, decorated nanoparticles [10] and spin filters [11], to name a few. Although the Fano theory was built on a scattering framework where the observable was the population on the con-

tinuum (i.e. the ionized electrons), the result continued to be applied (with remarkable success) to dissipative, non-scattering systems where the observable was not always the population in the continuum of states. As noted by A. E. Miroshnichenko in 2010, “*a suitable theory for a quantitative description of these cases is still lacking*” [5]. Not only is a justification of the use of a Fano profile important for the sake of rigor, but such a theory would make the connection between the Fano parameter q and the physical quantities of the system.

In this letter, we solve the dynamics of a quantum system with energy levels in a Fano like configuration but coupled to a bath which induces excited states relaxation described in the Born-Markov approximation, by the Liouville equation in Lindblad form [12] for the system density matrix evolution. In addition to the absorption cross-sections which is what the original Fano model considers, we also provide the equations to describe the full optical emission, that is the coherent Rayleigh and Raman scattering and the incoherent fluorescence.

Although our formalism is general and can be applied to a variety of systems, an important motivation is the type of architectures encountered in light harvesting systems [13, 14], where typically an atom or a molecule is adsorbed to a semiconductor surface. In most physical realizations of importance in solar energy research, the electronic ground state of this hybrid system is an isolated quantum state located in the semiconductor energy gap while the excited states can be considered as superposition of localized molecular excited states and delocalized semiconductor conduction band states [14, 15]. Evidence suggests that such a model with minor modifications could also account for molecules on metal nanoparticles [10, 16, 17]. Be it for solar energy applications,

electronic or sensors, there is strong evidence that the details of the interface distinguish functioning from non-functioning devices [18].

The energy levels of our model, along with the possible transitions, are shown in Figure 1. A discrete excited state $|e\rangle$ with energy ϵ_e is coupled to a continuum of states $|k\rangle$ with energy ϵ_k . These states can be reached from a ground state $|g\rangle$ through laser excitation. A sub-manifold (typically vibrational) $|\nu\rangle$ with energy ϵ_ν is included in the electronic ground state to open inelastic scattering channels as $|\nu\rangle \rightarrow |\nu'\rangle$. The Hamiltonian is:

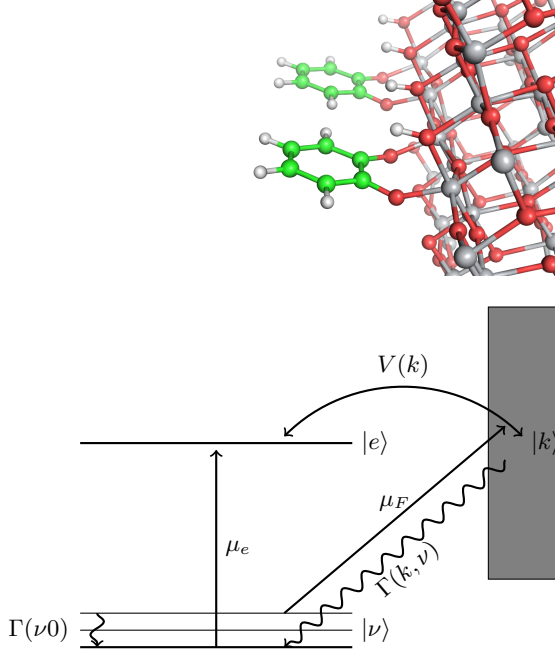


FIG. 1: Energy levels and transitions of a Fano model with dissipation, including a vibrational ground state manifold, a discrete excited state and a continuum (bottom). A particular realization of a Fano system with dissipation is a molecule adsorbed on a metal oxide semiconductor, here two catechol molecules on a (101) anatase TiO_2 surface (top)

$$\begin{aligned}
 H &= H_0 + H_V + H_F \\
 H_0 &= \sum_{\nu} \epsilon_{\nu} |\nu\rangle\langle\nu| + \epsilon_e |e\rangle\langle e| + \int dk \epsilon_k |k\rangle\langle k| \\
 H_V &= \int dk V(k) |e\rangle\langle k| + V^*(k) |k\rangle\langle e| \\
 H_F &= F \sum_{\nu} [\mu_{\nu e} \cos(\omega_L t) |\nu\rangle\langle e| + \mu_{\nu e}^* \cos(\omega_L t) |e\rangle\langle \nu|] \\
 &+ F \sum_{\nu} \int dk [\mu_{\nu k} \cos(\omega_L t) |\nu\rangle\langle k| + \mu_{\nu k}^* \cos(\omega_L t) |k\rangle\langle \nu|]
 \end{aligned} \tag{2}$$

where H_0 is the site Hamiltonian, H_V is the coupling of the excited state to the continuum, for simplicity, in the following, we will consider that $V(k) = \langle e|H_V|k\rangle$ is real.

H_F is the interaction with the incident radiation field of frequency ω_L , allowing transitions from the ground state to the discrete excited state $\nu \leftrightarrow e$ and to the continuum of states $\nu \leftrightarrow k$, $\mu_{ij} = \langle i|\mu|j\rangle$ is the transition dipole moment between states i and j and F is the field amplitude.

The originality of our model consists in taking into account a possible population relaxation of the continuum excited to the ground state at a rate $\Gamma(k, \nu)$. When the photo-excitation involves an electron, this relaxation is mainly the result of the electron-hole Coulombic attraction followed by the thermal relaxation through the phonons of the environment. We phenomenologically capture this dissipation process using a superoperator of Lindblad [12] form, which ensures the trace-preserving and complete positivity of the dynamical map, and solve the evolution of the density matrix with Liouville's equation:

$$\frac{\partial \rho}{\partial t} = \mathcal{L}(t)\rho \tag{4}$$

where $\mathcal{L}(t) = \mathcal{L}_H(t) + L^D$, with $\hbar \mathcal{L}_H = -i(\mathbb{1} \otimes H^T(t) - H(t) \otimes \mathbb{1})$, $L^D = L_k^D + L_{\text{vib}}^D + L_{\text{pure}}^D$

$$\begin{aligned}
 L_k^D &= \sum_{\nu} \int dk \Gamma(k, \nu) \left\{ A(k, \nu) \otimes A(k, \nu) \right. \\
 &\left. - \frac{1}{2} [1 \otimes A^\dagger(k, \nu) A(k, \nu) + A^\dagger(k, \nu) A(k, \nu) \otimes 1] \right\}, \tag{5}
 \end{aligned}$$

$$\begin{aligned}
 L_{\text{vib}}^D &= \sum_{\nu \neq 0} \Gamma_{\nu 0} \left\{ A(\nu, 0) \otimes A(\nu, 0) \right. \\
 &\left. - \frac{1}{2} [1 \otimes A^\dagger(\nu, 0) A(\nu, 0) + A^\dagger(\nu, 0) A(\nu, 0) \otimes 1] \right\} \tag{6}
 \end{aligned}$$

and

$$\begin{aligned}
 L_{\text{pure}}^D &= - \sum_{\nu} \gamma_{e\nu} [|e\rangle\langle e| \otimes |\nu\rangle\langle \nu| + |\nu\rangle\langle \nu| \otimes |e\rangle\langle e|] \\
 &- \sum_{\nu} \int dk \gamma_{k\nu} [|k\rangle\langle k| \otimes |\nu\rangle\langle \nu| + |\nu\rangle\langle \nu| \otimes |k\rangle\langle k|] \\
 &- \int dk \gamma_{ke} [|k\rangle\langle k| \otimes |e\rangle\langle e| + |e\rangle\langle e| \otimes |k\rangle\langle k|], \tag{7}
 \end{aligned}$$

where H^T denotes the transpose of H , $A(i, j) = |j\rangle\langle i|$ are the jump operators and $\Gamma(k, \nu)$ is the population relaxation rate from state $|k\rangle$ to $|\nu\rangle$. The superoperator L_{vib}^D relaxes the ground states vibrational manifold and $\Gamma_{\nu 0}$ is the population relaxation rate within the electronic ground state manifold. γ_{ij} are the pure dephasing rates for the ij coherence relaxations. We have used the isomorphism from the adjoint representation (also called the column form) to the tensorial product given by: $L\bar{\rho}R \rightarrow L \otimes R^T \rho$, where ρ is the column form of the matrix $\bar{\rho}$ through the correspondance: $|l\rangle\langle m| \leftrightarrow |l\rangle \otimes |m\rangle \equiv ||lm\rangle$ [19]. Non-radiative quenching can exist, from the electronic excited state $|e\rangle$ to the ground states $|\nu\rangle$, but it is excluded for simplicity, although its inclusion can be done trivially. In practice, the electronic coupling V induces a much faster transition than this relaxation mechanism.

The optical response, the absorption as well as the emission spectrum, is obtained through the Fourier transform of the field two-times correlation function :

$$C(t, \tau) = 2\epsilon_0 c \langle E_\theta^{(-)}(t) E_\theta^{(+)}(t + \tau) \rangle, \quad (8)$$

where $E_\theta^{(\pm)}(t)$ are the negative/positive frequency parts of the spherical polar component of the electric field, ϵ_0 and c are the vacuum permittivity and the light velocity, respectively. The emitted intensity at time t is given by $C(t, 0)$ and the spectral power density is obtained through the Fourier transform of $C(0, \tau)$. In the far field region, it can be shown that $C(t, \tau)$ is proportional to the dipole two-times correlation function [20]. Using the quantum regression theorem [21–23], the emitted light differential scattering cross-section can be written in the steady-state of the system as [24, 25]:

$$\frac{d^2\sigma}{d\Omega d(\hbar\omega)} = A(\theta) \times \sum_{a \in e} \sum_{b \in g} \mu_{ab}^2 \sum_{r \in g, e} \text{Re}[\rho_{ra} G_{ab,rb}(-i(\omega - \omega_L))], \quad (9)$$

with $A(\theta) = \frac{\omega^4 \sin^2 \theta}{I_{\text{in}} 8\pi^3 c^3 \epsilon_0 \hbar}$, $d\Omega$ the element of solid angle, I_{in} the incident laser intensity, θ the polar angle in spherical coordinates, μ_{ab} a transition dipole moment matrix element, ρ the steady state density matrix and $G(z) = (z\mathbb{1} - i\Omega_L - L)^{-1}$ the resolvent of the time-independent Liouvillian $L = e^{i\Omega_L t} \mathcal{L}(t) e^{-i\Omega_L t}$, in the rotating-wave approximation (RWA), which consists in removing resonant oscillating prefactors and discarding non resonant terms. The Ω_L matrix is a diagonal matrix with $\pm\omega_L$ for excited(ground)-ground(excited) coherences, and zero elsewhere. We focus on the weak field, steady-state, response because experimentally the Raman, Rayleigh and fluorescence spectra are taken at low intensities under continuous wave irradiation validating the RWA. In summary, in order to obtain the optical emission we need to calculate the resolvent and the steady-state density matrix, which we do next.

To obtain an explicit expression of $G(z)$, we separate L into a diagonal part L_0 , whose resolvent $G_0(z) = (z\mathbb{1} - i\Omega_L - L_0)^{-1}$ is trivial even for the continuous infinite component, and the remaining non-diagonal part. The non-diagonal elements correspond to the field H_F , the H_V coupling and the non-diagonal part of the relaxation $\Gamma(k, \nu) A(k, \nu) \otimes A(k, \nu)$. We first obtain the exact resolvent $G^M(z) = (z\mathbb{1} - i\Omega_L - L^M)^{-1}$ of the liouvillian describing the material part, without the field coupling, $L^M = L - L_{H_F} = L_0 + W$, by solving explicitly the Dyson equation:

$$G^M = G_0 + G_0 W G^M. \quad (10)$$

Then we obtain the full resolvent at the second order in the field as $G(z) \simeq G^M + G^M L_{H_F} G^M + G^M L_{H_F} G^M L_{H_F} G^M$.

The steady-state density matrix ρ is the kernel of the Liouvillian after the RWA is applied, that is $(-i\Omega_L - L)\rho = 0$, which is equivalent to $\rho = ||00\rangle + G^M(0) L_{H_F} \rho$, where $||00\rangle$ is the kernel of L^M . For low temperature we consider here, $||00\rangle$ is the ground state. ρ can also be expanded to all orders in the field as $\rho = \sum_{n=0}^{\infty} [G^M(0) L_{H_F}]^n ||00\rangle$.

The above-mentioned steps are enough to calculate the optical response to the second order of the incident field which is the lowest order required for linear spectroscopy observables. For arbitrary model parameters $V(k)$, $\Gamma(k, \nu)$ and energy density of state $n(k) = \frac{dk}{dE}$, using the procedure outlined in Eqs. (9) (10) (3) and (4), we have obtained integral equations for the optical response which can be used for efficient numerical calculations. However, explicit expressions can be obtained under certain approximations. For many materials, the wideband approximation which considers that the model parameters related to the continuum are k -independent, can faithfully reproduce experimental measurements. It is also the approximation which allows a closed analytic form in the original Fano problem [3]. We introduce the notation $\Gamma_{c\nu} = \Gamma(k, \nu)$ and $\mu_{\nu c} = \mu_{\nu k}$ for the k -independent parameters and present the analytical results for a wideband continuum.

A straightforward but tedious calculation [26] yields all the terms needed to calculate the optical response (Eq 9), in the wide band approximation. Light-matter interaction can be divided into absorption, and emission and their expressions are the main results of this paper. For the absorption, we have $\frac{I_{\text{in}}}{I_{\text{em}}} = \frac{\pi n F^2 \mu_{0c}^2}{2\hbar(\Gamma_{c0} + \Gamma_{c1})} \mathcal{E}(\epsilon; q, \eta)$ with

$$\mathcal{E}(\epsilon; q, \eta) = \left[\frac{(q + \epsilon)^2}{\epsilon^2 + 1} + \eta \frac{q^2 + 1}{\epsilon^2 + 1} \right], \quad (11)$$

and where I_{em} is the full emitted light intensity, $\epsilon = (\hbar\omega_L - E_e)/(n\pi V^2)$, $q = \mu_{0e}/(n\pi V \mu_{0c})$ and $\eta = \hbar(\Gamma_{c0} + \Gamma_{c1})/(4\pi n V^2)$. We note that ϵ and q are the parameters of the original Fano model, while η is an additional parameter that expresses the population relaxation rate in units of the discrete-continuum transfer rate $\gamma = \pi n V^2/\hbar$. When $\eta \rightarrow 0$ the absorption profile is exactly a Beutler-Fano one, but when $\eta \neq 0$ there is an additional Lorentzian contribution.

The emission can be separated into two processes: coherent scattering (Rayleigh and Raman), and incoherent emission (fluorescence), which relies on non-zero occupation of the excited states. For the coherent scattering differential cross section:

$$\frac{d^2\sigma^{(c)}}{d\hbar\omega d\Omega} = A(\theta) \sum_{\nu} R_{\nu}^c(\omega) \mathcal{E}_{\nu}^c(\epsilon; q, \eta) \quad (12)$$

where $R_{\nu}^c(\omega) = \frac{1}{\pi\hbar} \frac{\Gamma_{\nu 0}}{(\omega - \omega_L + E_{\nu}/\hbar)^2 + (\Gamma_{\nu 0})^2}$ and

$$\mathcal{E}_{\nu}^c(\epsilon; q, \eta) = B \left\{ \frac{(\epsilon + q)^2}{\epsilon^2 + 1} + \eta \frac{\mu_{\nu e}^2}{n\mu_{\nu c}^2} \frac{q^2 + 1}{\epsilon^2 + 1} \right\} \quad (13)$$

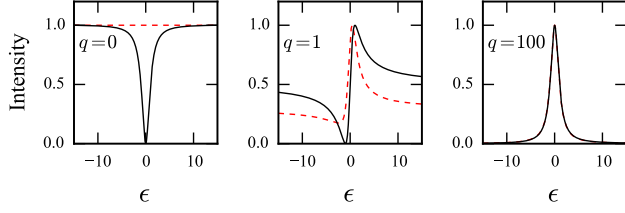


FIG. 2: Characteristic function for absorption or Raman emission for $\eta = 0$ (solid black) and $\eta = 1$ (red dashed) for $q = 0, 1, 100$ (intensities are normalized).

with $B = \frac{\pi^2 n^2 F^2 \mu_{0c}^2 \mu_{\nu c}^2}{2\hbar(\Gamma_{c0} + \Gamma_{c1})}$. $R_\nu(\omega)$ gives the lineshape and as expected, for a coherent scattering process, its linewidth does not depend on the excited states lifetime. $\mathcal{E}_\nu^c(\epsilon; q, \eta)$ gives the integrated intensity of the emission peak, often called the excitation profile. $\nu = 0$ and 1 corresponds to Rayleigh and Raman Stokes lines respectively. To avoid singularities the value of Γ_{00} is taken as a very small real number which physically represents the laser linewidth.

Without the presence of pure dephasing, the fluorescence vanishes. Its inclusion gives a fluorescence spectrum which has also a modified Fano profile. For pure dephasings such that $\gamma_{ke} = \gamma_{k0} \neq 0$ and $\gamma_{k1} \neq 0$, $\gamma_{e\nu} \neq 0$, we obtain $\frac{d^2 \sigma^{(f)}}{d\hbar\omega d\Omega} = \sum_\nu S_\nu^{(f)}(\omega)$, with:

$$S_\nu^f(\omega) = A(\theta) [C R_\nu^{f,e}(\omega) \mathcal{E}_\nu^{f,e}(\tilde{\epsilon}; q, \eta) + D R_\nu^{f,c}(\omega) \mathcal{E}_\nu^{f,c}(\tilde{\epsilon}; \tilde{q}, \eta)] \quad (14)$$

where $R_\nu^{f,e}(\omega) = \frac{1}{\pi} \frac{n\pi V^2 + \hbar\Gamma_{\nu 0} + \hbar\gamma_{e\nu}}{(\hbar\omega - E_e + E_\nu)^2 + (n\pi V^2 + \hbar\Gamma_{\nu 0} + \hbar\gamma_{e\nu})^2}$, $R_\nu^{f,c}(\omega) = \frac{1}{\pi\hbar} \frac{\Gamma_{c0} + \Gamma_{c1} + \Gamma_{\nu 0} + \gamma_{k\nu} + \gamma_{k0}}{(\hbar\omega - \omega_L + E_\nu/\hbar)^2 + (\Gamma_{c0} + \Gamma_{c1} + \Gamma_{\nu 0} + \gamma_{k\nu} + \gamma_{k0})^2}$ and

$$\mathcal{E}_\nu^{f,e}(\tilde{\epsilon}; q, \eta) = \left(\frac{n\pi V^2}{n\pi V^2 + \hbar\gamma_{e0}} \right)^2 \times \eta \frac{q^2 + 1}{\tilde{\epsilon}^2 + 1},$$

$$\mathcal{E}_\nu^{f,c}(\tilde{\epsilon}; \tilde{q}, \eta) = \frac{(\tilde{\epsilon} + \tilde{q})^2}{\tilde{\epsilon}^2 + 1} + \frac{\gamma_{e0}^2}{(n\pi V^2/\hbar + \gamma_{e0})^2} \frac{1}{\tilde{\epsilon}^2 + 1}, \quad (15)$$

with $C = \frac{\pi^2 n^2 F^2 \mu_{0c}^2 \mu_{\nu e}^2 \gamma_{e\nu}}{\Gamma_{c0} + \Gamma_{c1}}$, $D = \frac{C\gamma_{e0} + \gamma_{c1}}{\gamma_{e\nu}}$, $\tilde{\epsilon} = (\hbar\omega_L - E_e)/(n\pi V^2 + \hbar\gamma_{e0})$ and $\tilde{q} = q(n\pi V^2)/(n\pi V^2 + \hbar\gamma_{e0})$. The first term of Eq. (14) can be attributed to the emission from the excited state $|e\rangle$. The width of its lineshape $R_\nu^{f,e}(\omega)$ is given by the sum of the population and coherences relaxation rate in addition to $n\pi V^2/\hbar$. Its corresponding excitation profile $\mathcal{E}_\nu^{f,e}(\tilde{\epsilon}; q, \eta)$ as a function of $\tilde{\epsilon}$ is a Lorentzian. The second term of Eq. (14) corresponds to the emission from the continuum. Its excitation profile $\mathcal{E}_\nu^{f,c}(\tilde{\epsilon}; \tilde{q}, \eta)$ as a function of $\tilde{\epsilon}$ is a modified Fano profile.

Figure 2 shows normalized excitation profiles as given by Eq. (11), for several values of q and η . As $\eta \rightarrow 0$ (which corresponds to $\Gamma_{c1} + \Gamma_{c0} \gg 4\pi nV^2$), the curve approaches the standard Fano profile while $\eta = 1$ shows the Fano with a Lorentzian contribution for different values of the q parameter.

Fitting the optical response of a dissipative system with the original Fano profile $f(\epsilon, q)$ given by Eq. (1),

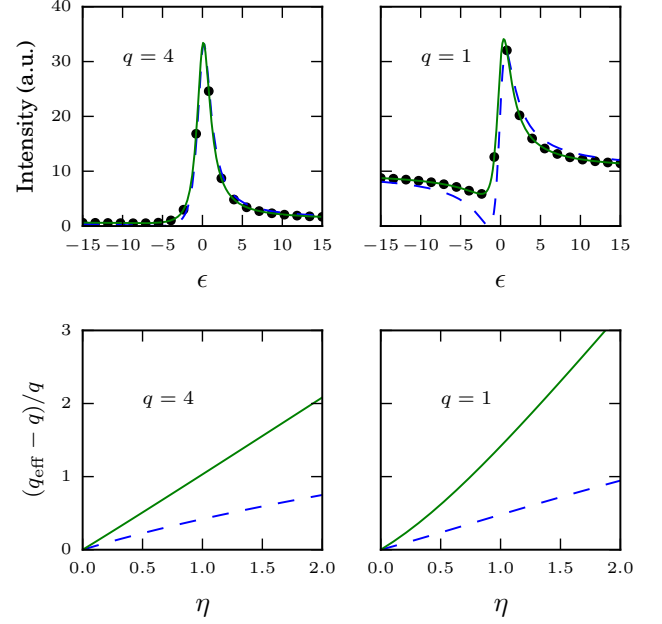


FIG. 3: Comparison between different Fano models. Top: fits of the profile presented in this paper Eq. (11) with $q = 4$ and 1 and $\eta = 1$ by a standard (blue dashed) or a shifted Fano profiles (solid green). Bottom: relative difference between the extracted q_{eff} and the actual q value for the standard (blue dashed) or the shifted Fano profiles (solid green).

provides an effective value q_{eff} which can be different from its actual value q depending on η . Figure 3 shows data points of the profile given by Eq. (11) with $q = 1$ and $q = 4$, and $\eta = 1$. We carry out two fits to this data, one with a standard Fano model $f(\epsilon, q)$, and one with a shifted Fano model: $g(\epsilon; q_{\text{eff}}, D, N) = \frac{1}{N} [f(\epsilon, q_{\text{eff}}) + D]$, where D is the shift and N a normalisation factor. The relative difference $\frac{q - q_{\text{eff}}}{q}$, between the fit parameter q_{eff} and the actual q is shown in the graphs below. For moderately large values of the parameter (here shown $q = 4$), a standard and the shifted Fano fits both reproduce successfully the data. However, as shown in the graph below, the extracted q_{eff} parameters can be off by a factor of two at $\eta = 1$. These values of q are in the range of those reported in [10]. For smaller values of q , the standard Fano fit does not reproduce well the data. For the shifted Fano profile, however, it can be shown [26] that we can always express the parameters q and η as a function of the 3 parameters (q_{eff}, N, D) such that our profile $\mathcal{E}(\epsilon; q, \eta)$ given by Eq. (11) matches exactly $g(\epsilon; q_{\text{eff}}, N, D)$, for all ϵ . Thus giving always an exact match between the fit and fitted curve but with $q_{\text{eff}} \neq q$.

We expect that the equations will motivate the experimentalist to extract system parameters from routine optical spectroscopies which would otherwise not be accessible, characterizing with increasing precision the discrete-

continuum interface both relevant in devices and interesting from a fundamental standpoint. Furthermore, our model opens a plethora of applications: optical response beyond the wide-band approximation which breaks down near the edges of conduction bands, strong field effects relevant for plasmonics, generalization to time-dependent laser pulses sequences relevant to non-linear 2D spectroscopy and application to real systems with the help of DFT.

Acknowledgements This work was financially supported by project NSF-ANR (ANR-11-NS04-0001 FRAMOLSENT program, NSFCHE-112489). D.F.S. acknowledges the Research in Paris program for a fellowship.

-
- [1] H. Beutler, Zeitschrift für Physik **93**, 177 (1935).
 - [2] U. Fano, Il Nuovo Cimento **12**, 154 (1935).
 - [3] U. Fano, Phys. Rev. **124**, 1866 (1961).
 - [4] K. O. Friedrichs, Commun. Pure Appl. Math. **1**, 361 (1948).
 - [5] A. E. Miroshnichenko, S. Flach, and Y. S. Kivshar, Rev. Mod. Phys. **82**, 2257 (2010).
 - [6] M. Rahmani, B. Luk'yanchuk, and M. Hong, Laser & Photonics Reviews **7**, 329 (2013).
 - [7] T. Pakizeh, C. Langhammer, I. Zori, P. Apell, and M. Kll, Nano Lett. **9**, 882 (2009).
 - [8] B. Lukyanchuk, N. I. Zheludev, S. A. Maier, N. J. Halas, P. Nordlander, H. Giessen, and C. T. Chong, Nat. Mater. **9**, 707 (2010).
 - [9] C. W. Hsu, B. G. DeLacy, S. G. Johnson, J. D. Joannopoulos, and M. Soljacic, Nano Lett. **14**, 2783 (2014).
 - [10] J. R. Lombardi and R. L. Birke, J. Phys. Chem. C **114**, 7812 (2010).
 - [11] J. F. Song, Y. Ochiai, and J. P. Bird, Appl. Phys. Lett. **82**, 4561 (2003).
 - [12] G. Lindblad, Communications in Mathematical Physics **48**, 119 (1976).
 - [13] B. O'Regan and M. Graetzel, Nature (London) **353**, 737 (1991).
 - [14] A. Hagfeldt, G. Boschloo, L. Sun, L. Kloo, and H. Pettersson, Chem. Rev. **110**, 6595 (2010).
 - [15] W. R. Duncan and O. V. Prezhdo, Annu. Rev. Phys. Chem. **58**, 143 (2007).
 - [16] J. R. Lombardi and R. L. Birke, J. Phys. Chem. C **112**, 5605 (2008).
 - [17] J. Lombardi and R. Birke, Acc. Chem. Res. **42**, 734 (2009).
 - [18] E. Galoppini, Coord. Chem. Rev. **248**, 1283 (2004).
 - [19] T. F. Havel, Journal of Mathematical Physics **44**, 534 (2003).
 - [20] S. Mukamel, *Principles of nonlinear optical spectroscopy* (Oxford University Press, 1995).
 - [21] M. Lax, Phys. Rev. **129**, 2342 (1963).
 - [22] G. Agarwal, in *Quantum Optics*, Springer Tracts in Modern Physics, Vol. 70 (Springer Berlin Heidelberg, 1974) pp. 1–128.
 - [23] C. Cohen-Tannoudji, J. Dupont-Roc, and G. Grynberg, *Processus d'interaction entre photons et atomes*, Savoirs Actuels (EDP Sciences, 2012).
 - [24] P. Johansson, H. Xu, and M. Käll, Phys. Rev. B **72**, 1 (2005).
 - [25] H. Xu, X.-H. Wang, M. Persson, H. Xu, M. Käll, and P. Johansson, Phys. Rev. Lett. **93**, 1 (2004).
 - [26] See Supplemental Material at.